General Disclaimer

One or more of the Following Statements may affect this Document

- This document has been reproduced from the best copy furnished by the organizational source. It is being released in the interest of making available as much information as possible.

- This document may contain data, which exceeds the sheet parameters. It was furnished in this condition by the organizational source and is the best copy available.

- This document may contain tone-on-tone or color graphs, charts and/or pictures, which have been reproduced in black and white.

- This document is paginated as submitted by the original source.

- Portions of this document are not fully legible due to the historical nature of some of the material. However, it is the best reproduction available from the original submission.

(NASA-CR-157890) A STUDY OF MULTIPLE-SHAKER MODAL SURVEY TESTING Final Report, Feb. 1976 - Sep. 1978 (Virginia Polytechnic Inst. and State Univ.) 44 p HC A03/MF A01 CSCL 20K G3/39

N79-10447

Unclas 33886

FINAL REPORT
February 1976 - September 1978

NASA Langley Research Center
Research Grant NSG 1276

A STUDY OF MULTIPLE-SHAKER MODAL SURVEY TESTING

William L. Hallauer, Jr.
Department of Aerospace and Ocean Engineering
Virginia Polytechnic Institute and State University
Blacksburg, Virginia 24061

FINAL REPORT

A STUDY OF MULTIPLE-SHAKER MODAL SURVEY TESTING*

I. Summary

This research has been concerned with methods of structural dynamic testing. The principal objective has been to examine and to assess the practical value of a method of multiple-shaker sinusoidal modal vibration testing known as Asher's method. Numerical studies which simulate the application of Asher's method and a unique experimental implementation of the method have been completed. Another objective of the research has been to develop and to demonstrate with numerical simulation a quantitative method for determining from transfer function data the number of dominant modes of vibration in sinusoidal structural response.

II. Studies of Asher's Method

The first report on numerical simulation of Asher's method was the Master's thesis by Stafford [1]. Simulated modal testing on a relatively simple mathematical structural model was examined in considerable detail. Stafford's model is a cantilevered plane grid structure having five degrees of freedom, a pair of closely spaced modes, and hysteretic damping which does not couple the undamped normal modes. The next report on numerical simulation was the Master's thesis by Shostak [2]. Shostak's mathematical models are similar to Stafford's but have viscous damping which does couple the undamped normal modes. The final and most significant report on numerical simulation was the paper by Hallauer and Stafford, which was presented

---

*The NASA Technical Officer for this grant is Mr. Robert Miserentino, NASA Langley Research Center.

at a technical conference [3], and published in a journal [4]. The abstract for this paper follows.

> The method proposed by Asher for structural dynamic modal testing by multiple-shaker sinusoidal excitation is reviewed, and its theory and application are discussed in detail. Numerical results from simulated modal testing on mathematical structural models are presented to illustrate the strengths and weaknesses of the method. The characteristics of these models include damping which couples the normal modes and closely spaced modes. Numerical techniques required for implementation of the method are described. A procedure is suggested for replacing actual mechanical tuning with calculations employing transfer function data.

The experimental study of Asher's method was conducted in the Structural Dynamics Research Laboratory of NASA Langley Research Center. The objective was to develop and test the software and procedures for application of the method with the use of the SDRL's programmable Hewlett-Packard 5451B Fourier Analyzer System with Modal Analysis Option. The most detailed report on this experimental study is the Master's thesis being prepared by R. R. Gold, which will be submitted to VPI & SU in late 1978 or early 1979. Also, a technical paper by R. R. Gold and W. L. Hallauer, Jr. is being submitted for presentation at the 25th International Instrumentation Symposium (May 7 - 10, 1979 in Anaheim, California) and publication in the symposium proceedings. This paper is entitled "Implementation of Asher's Method of Modal Testing on a Fourier-Analysis/Modal-Test System", and its abstract follows.

> A software package for application of Asher's method has been implemented on a modern Fourier analyzer system. This combination is unusual since the original form of Asher's method involves multiple-shaker, sinusoidal-dwell mechanical tuning, whereas the more recent method of analysis-based modal testing employs single-point transient or random excitation, with modal separation attempted by curve fitting of FFT-calculated transfer functions. The technique described uses FFT and curve-fitting capabilities to produce an analytical form of multiple-shaker

tuning. For evaluation of this technique, a model having two modes with almost identical natural frequencies was designed mathematically and fabricated. Evaluation with numerically simulated data for this model demonstrated that the technique works extremely well in principle. However, actual testing of the model produced such poor transfer function data that practical evaluation was not possible.

The principal application of multiple-shaker modal testing is in the difficult task of separating and correctly characterizing closely spaced modes of vibration. In order to assess the practical value of Asher's method, it has therefore been necessary to have available relatively simple structural models with closely spaced modes. It is very difficult to create such models by intuition or trial and error, so a quantitative design method has been developed and is described in detail in the paper by Hallauer et al [5]. The abstract for this paper follows.

Vehicle structures often have closely spaced modes of vibration within the frequency spectrum of applied loads. Such modes are important since they tend to be the source of vibration problems. In order to study the effects that closely spaced modes have on structural response in such situations as modal testing and self-excited vibrations, it is useful to be able to design a mathematical structural model having closely spaced modes. In this paper, a method for designing such a model is presented and illustrated with examples. Given a reference model with specified geometry and degrees of freedom, the lumped inertias and stiffnesses of the model are perturbed in such a manner as to force together two of its natural frequencies. With a slight alteration, the method is also applicable to the inverse problem of separating undesirable closely spaced modes which appear in a structural design.

An interim report of this research (Semi-Annual Progress Report, May-November 1977, Research Grant NSG 1276) stated that a NASA Contractor Report would be published with the title "A Method for Modal Tuning by Multiple-Shaker Sinusoidal Excitation: Theory and Numerical Simulation". The CR has not been and will not be published. All the material that was to have been included in the CR is available in references [4] and [5].

III. Determining the Number of Dominant Vibration Modes

Very significant progress has been made in the development and demonstration of a quantitative method for determining from transfer function data the number of dominant modes. The first report on this subject was the Master's thesis by Franck [6]. The research was also presented at a technical conference in a paper by Hallauer and Franck [7]. Finally, a detailed and comprehensive paper by W. L. Hallauer, Jr. and A. Franck has been submitted for publication in late 1979 in the 48th Shock and Vibration Bulletin. In order to make this paper available prior to its publication, it has been included as the Appendix to this report.

REFERENCES

1. J. F. Stafford, "A Numerical Simulation of Multiple-Shaker Modal Testing", Master's thesis, VPI & SU, July 1976.

2. A. G. Shostak, "A Numerical Simulation of Modal Testing on a Structure with Viscous Damping", Master's thesis, VPI & SU, November 1977.

3. W. L. Hallauer, Jr., and J. F. Stafford, "On the Distribution of Shaker Forces in Multiple-Shaker Modal Testing", 48th Shock and Vibration Symposium, Huntsville, Alabama, October 18-20, 1977.

4. W. L. Hallauer, Jr. and J. F. Stafford, "On the Distribution of Shaker Forces in Multiple-Shaker Modal Testing", The Shock and Vibration Bulletin, 48 (1), pp. 49-63, September 1978.

5. W. L. Hallauer, Jr., T. A. Weisshaar and A. G. Shostak, "A Simple Method for Designing Structural Models with Closely Spaced Modes of Vibration", Journal of Sound and Vibration, 61 (2), November 1978.

6. A. Franck, "A Method for Determining the Number of Dominant Modes in Sinusoidal Structural Response", Master's thesis, VPI & SU, May 1978.

7. W. L. Hallauer, Jr., and A. Franck, "On Determining the Number of Dominant Modes in Sinusoidal Structural Response", 49th Shock and Vibration Symposium, Washington, D.C., October 17-19, 1978.

APPENDIX

ON DETERMINING THE NUMBER OF DOMINANT MODES IN SINUSOIDAL STRUCTURAL RESPONSE

W. L. Hallauer, Jr. and A. Franck

ABSTRACT

This paper addresses the problem of using structural dynamic transfer function data to determine the number of vibration modes dominant in response at a given frequency. If two or more modes are closely spaced or if response is influenced strongly by distant modes, then the number of dominant modes may not be evident from examination of transfer function plots, and quantitative methods may be required. Two relatively simple methods which have been used previously are reviewed, and a more effective new method, called the vector-fit method, is described in detail. Applications of these methods are given with the use of numerically simulated transfer functions data.

I. INTRODUCTION

At any particular frequency of excitation, the steady-state sinusoidal response of a structure is dominated by only a few of its indefinitely large number of vibration modes. The objective of modal testing is to measure specific parameters of the dominant modes such as natural frequencies, damping values, and mode shapes. When applicable, the best method for determining the number of dominant modes in a frequency band is simply to count resonance peaks on transfer function plots. In such a situation, modal parameters can then be calculated rather easily by modern curve-fitting algorithms, most of which require the number of dominant modes as an input value. However, if two or more modes are closely spaced, or if response is influenced strongly by modes whose resonances are outside the frequency band of interest, then peak counting may not reveal the true number of dominant modes, and subsequent curve fitting of transfer function data may produce incorrect modal parameters and/or miss modes entirely. But a quantitative method for determining the number of dominant modes may succeed where peak counting fails. If such a method should reveal the presence of previously undetected modes, then careful curve fitting or some other modal testing technique, such as multiple-shaker tuning, might successfully separate the modes.

The problem of determining the number of dominant modes was discussed extensively some years ago in connection with the number of shakers required to separate modes in multiple-shaker modal testing. Traill-Nash [1] introduced the "effective number of degrees of freedom" at a given frequency, which he defined as being the number of motion coordinates required to represent with accuracy structural response at that frequency. He concluded that the number of shakers must equal or exceed the effective number of degrees

of freedom. Bishop and Gladwell [2] suggested a relationship between Traill-Nash's effective number of degrees of freedom and the number of dominant modes; subsequently, Asher [3] implicitly equated these two numbers. He then stated, in effect, that the number of shakers required equals the number of dominant modes. This contention is not generally true; the number of distinct generalized force distributions must equal the number of dominant modes, but there is no necessary relationship between the number of generalized force distributions and the number of discrete forces. Nonetheless, Asher made a significant contribution by proposing probably the first quantitative methods to determine the number of dominant modes by analysis of transfer function data.

This paper describes the theoretical basis for such a quantitative method, reviews the methods discussed by Asher, proposes a new and more effective method, and illustrates these methods with the use of numerically simulated transfer function data.

II. THEORETICAL BACKGROUND

Consider a linear structure discretized to n degrees of freedom, the time-dependent responses of which are elements of the n x 1 column matrix $\underset{\sim}{x}$. (Notation is listed at the end of the paper.) The governing matrix equation of motion is

$$[m]\,\ddot{\underset{\sim}{x}} + [c]\,\dot{\underset{\sim}{x}} + [k]\,\underset{\sim}{x} = \underset{\sim}{f} \qquad (1)$$

where [m], [c], and [k] are the n x n inertia, damping, and stiffness matrices, respectively, and $\underset{\sim}{f}$ is the column matrix of time-dependent forcing. We specify that all forces vary sinusoidally at the same frequency, ω, and that all have 0° or 180° phase,

$$\underset{\sim}{f} = \underset{\sim}{F} \cos \omega t = \mathrm{Re}\left\{\underset{\sim}{F}\, e^{i\omega t}\right\} \qquad (2a)$$

After starting transients have decayed away, response is steady-state sinusoidal,

$$\underset{\sim}{x} = \mathrm{Re}\left\{ \underset{\sim}{\chi}\, e^{i\omega t} \right\} \tag{2b}$$

where the elements of amplitude vector $\underset{\sim}{\chi}$ are generally complex, reflecting phase differences between excitation and response. The linear, frequency-dependent relationship between excitation amplitude and complex response amplitude is defined by the n x n transfer function matrix $[H(\omega)]$,

$$\underset{\sim}{X} = [H(\omega)]\, \underset{\sim}{F} \tag{3}$$

The standard real modal analysis solution of equation (1) for $[H(\omega)]$ begins with calculation of the real undamped natural frequencies ω_r, r = 1, 2, ···, n, and the associated real mode shape vectors $\underset{\sim}{\phi}_r$, which are the columns of modal matrix $[\phi]$ (Meirovitch [4]). Subsequently, response coordinates X_i are transformed into normal coordinates which diagonalize the mass and stiffness matrices of equation (1); then the normal coordinates are calculated by matrix inversion, and $\underset{\sim}{X}$ is calculated from the normal coordinate solution in the form

$$\underset{\sim}{X} = [\phi]\, [S(\omega)]\, \underset{\sim}{F}$$

where $[S(\omega)]$ is an n x n complex matrix. Hence, the transfer function matrix is

$$[H(\omega)] = [\phi]\, [S(\omega)]$$

and any column, say the jth, of $[H(\omega)]$ can be written as

$$\underset{\sim}{H}_j(\omega) = \sum_{r=1}^{n} S_{rj}(\omega)\, \underset{\sim}{\phi}_r, \quad j = 1,2,\cdots,n \tag{4}$$

Thus, each column of the transfer function matrix can be expressed as a summation of the n linearly independent mode shape vectors. If we consider some subset p < n of degrees of freedom and define the corresponding p x 1 incomplete

jth transfer function column as $\underset{\sim}{H}_j^*(\omega)$, then equation (4) gives

$$\underset{\sim}{H}_j^*(\omega) = \sum_{r=1}^{n} S_{rj}(\omega) \; \underset{\sim}{\phi}_r^* \; , \; j = 1, 2, \ldots, n \qquad (5)$$

where the degrees of freedom included in each p x 1 incomplete mode shape vector $\underset{\sim}{\phi}_r^*$ are the same as those included in $\underset{\sim}{H}_j^*$. Although the summation in equation (5) extends over all modes, only p of the n $\underset{\sim}{\phi}_r^*$ vectors are independent.

If damping matrix [c] were to couple the undamped normal modes (i.e., if $[\phi]^t$ [c] [ϕ] were not diagonal), then the use of undamped normal modes as outlined above would be computationally inefficient, and we would probably solve for the transfer function matrix with an appropriate complex modal analysis employing complex eigenvalues and mode shape vectors. Nevertheless, the solution for each column of the transfer function matrix could still be expressed in the forms of equations (4) and (5), that is, as linear summations of n mode shape vectors, where in this case the $\underset{\sim}{\phi}_r$ would be complex vectors. The important fact, expressed in the language of matrix theory, is that each transfer function column $\underset{\sim}{H}_j$ is an element in the n-dimensional vector space spanned by the n mode shape vectors, whether they be real or complex; similarly, each incomplete column $\underset{\sim}{H}_j^*$ is an element in the p-dimensional vector space spanned by any p linearly independent incomplete mode shape vectors.

A useful general characteristic of structural dynamic behavior is that very few of a structure's many vibration modes are sensitive to excitation at any given frequency. These few modes then dominate the response at that frequency. If there are q such dominant modes at frequency ω, then the mathematical statements of their dominance, from equations (4) and (5), are

$$\underset{\sim}{H}_j(\omega) \simeq \sum_q S_{rj}(\omega) \ \underset{\sim}{\phi}_r, \ j = 1, 2, \ldots, n \tag{6}$$

$$\underset{\sim}{H}^*_j(\omega) \simeq \sum_q S_{rj}(\omega) \ \underset{\sim}{\phi}^*_r, \ j = 1, 2, \ldots, n \tag{7}$$

where $\sum_q$ denotes summation over only the q dominant modes. In equation (6), the q n x 1 mode shape vectors associated with the dominant modes generate a q-dimensional subspace of the original n-dimensional vector space. The approximate equality in equation (6) means that each $\underset{\sim}{H}_j(\omega)$ column can, with small error, be considered an element of the subspace. In equation (7), the p x 1 incomplete mode shape vectors associated with the dominant modes generate a q-dimensional subspace of the original p-dimensional vector space, provided that $p \geq q$. Again, the approximate equality means that each $\underset{\sim}{H}^*_j(\omega)$ column is approximately an element of the subspace.

Most current methods of modal testing are capable of measuring incomplete transfer function column vectors over a frequency band of interest. The jth column $\underset{\sim}{H}^*_j$ represents physically the complex response amplitude of motion sensors at p stations on the test structure due to sinusoidal forcing excitation of unit amplitude at the jth station, which does not necessarily coincide with any of the motion sensor stations. If excitation is applied successively to k different stations, then vectors $\underset{\sim}{H}^*_j$, j = 1, 2, ...k, can be measured. They are the columns of the p x k incomplete transfer function matrix $[H^*]$. (It is generally impossible to measure the complete matrix [H], since a continuous structure has an indefinitely large number of degrees of freedom.)

If the structure being tested responds linearly, then each $\underset{\sim}{H}^*_j$ column is represented mathematically by equation (7), which, therefore, is the basis of the methods discussed in Section III below for determining the number of

dominant modes from experimental transfer function data. Each method estimates the number q of dominant vectors ϕ_r^* in equation (7), given k experimental $p \times 1$ vectors H_j^*.

One practical requirement for the correct use of equation (7) in the present context is immediately evident: since p must exceed q, as discussed above, the test engineer must guess an upper bound q_{max} for the number of dominant modes likely to be encountered, and then he must install more than q_{max} distinct motion sensors. This requirement does not present a significant practical obstacle, since q_{max} for most structures should be on the order of ten or less. It is assumed in the remainder of the paper that the number of motion sensor measurements available for analysis is always greater than the number of dominant modes.

In vehicle modal testing, it is usually feasible to install a substantial number of motion sensors, but the number of exciters or excitation stations is often much smaller due to practical limitations. Hence, we assume that $k \leq p$ in most of what follows.

III. QUANTITATIVE METHODS FOR DETERMINING THE NUMBER OF DOMINANT MODES

III.1 TRANSFER FUNCTION DETERMINANT METHOD

This method involves analysis of square transfer function matrices, which are formed by the use of only k of the p available motion sensor measurements. Thus, $[H^*]$ is a $k \times k$ matrix. If, in the first case, the number of exciters is less than or equal to the number of dominant modes, $k \leq q$, then according to equation (7), the k columns of $[H^*]$ generally will be linearly independent: hence $[H^*]$ will be non-singular and its determinant will be non-zero,

det [H*] ≠ 0 for k ≤ q. But if the number of exciters is increased until it just exceeds the number of dominant modes, k = q + 1, then the k columns will be approximately dependent, so that [H*] will be nearly singular and its determinant will be close to zero, det [H*] ≈ 0 for k > q. The strategy for application of this method, therefore, is to add rows and columns of data to the transfer function matrix in unit steps until the value of k is found for which det [H*] ≈ 0; then the conclusion is that q = k - 1.

This is a very simple method to apply, but it has some deficiencies. First, transfer function determinants are complex, so one must assess the possibly non-monotonic progression toward zero of a sequence of complex numbers. Second, the restriction to square transfer function matrices is undesirable because it prevents the use of all available motion sensor data. Both of these deficiencies are eliminated with little additional effort by the use of the Gram determinant method described below, so there appears to be no reason to develop further or test the transfer function determinant method. We note that Ibrahim and Mikulcik [5] employed a similar method, but with filtered transient response data, and found it quite satisfactory.

III. 2 GRAM DETERMINANT (GRAMIAN) METHOD

This method involves analysis of a rectangular p x k transfer function matrix, [H*]. The Gram matrix of [H*] is defined to be a matrix product,

$$[G_k] = [\bar{H}^*]^t [H^*]$$

where the overbar indicates complex conjugacy. By this definition, the Gram matrix is a k x k Hermitian matrix. The Gram determinant, or Gramian, is

defined to be

$$G^{(k)} = \det [G_k]$$

It can be proved that the Gramian is real and non-negative.

The Gramian of a transfer function matrix is a quantitative measure of the degree of linear dependence of the column vectors, $\underset{\sim}{H}^*_j$, $j = 1, 2, \ldots, k$. Specifically, the set of vectors is linearly dependent if and only if the Gramian is zero (Hildebrand [6]). Moreover, it is reasonable to expect that if the set of vectors is almost but not precisely linearly dependent, then the Gramian should be nearly zero. As is discussed in Section III.1, any q or fewer columns of [H*] generally are linearly independent and, hence, have non-zero Gramians, $G^{(k)} > 0$ for $k = 1, 2, \ldots, q$. But any set of more than q columns will be approximately dependent and have very small or zero Gramians, $G^{(k)} \approx 0$ for $k \geq q + 1$. Therefore, the basic strategy for application of this method is to add columns of data to the transfer function matrix in unit steps until the value of k is found for which $G^{(k)} \approx 0$; then, the conclusion is that $q = k - 1$.

It is necessary in applying this method to separate the change in Gram determinant value due to change in degree of linear dependence from that due simply to change in determinant size. If, for example, all Gram matrix elements are numerically of order 10^{-2}, then, without change in degree of linear dependence, $G^{(1)}$ will be of order 10^{-2}, $G^{(2)}$ of order 10^{-4}, $G^{(3)}$ of order 10^{-6}, and so forth. This characteristic of determinants will obviously mask the Gramian test for linear dependence unless Gram matrix elements are of order 1. In applications of the Gramian method, the authors have attempted to minimize the masking by normalizing each column of [H*] so that the corresponding diagonal

element of the Gram matrix is 1, i.e., $(\underset{\sim}{H}_j^*, \underset{\sim}{H}_j^*) = 1$, $j = 1,2,\ldots,k$, where $\underset{\sim}{H}_j^*$ here denotes the normalized column rather than the original column in physical units. The numerical results of Section IV.3 suggest that this ad hoc measure is effective in filtering out Gramian variation with Gram matrix size.

Asher [3] described and discussed both the transfer function determinant and the Gram determinant methods. He recognized that in applying either method, one might find it difficult to decide how small a generally non-zero determinant value must be in order to indicate linear dependence correctly. The numerical results of Section IV.3 confirm that the absence of a definite smallness criterion is indeed a weakness of the Gramian method. Even though all Gramian values are referenced to $G^{(1)} = 1$ by virtue of the normalization procedure described above, examples for different situations show Gramian values $G^{(q+1)}$ of orders 10^{-1}, 10^{-2}, and even 10^{-3}.

Another deficiency of the Gramian method is that it can correctly indicate linear dependence, yet underestimate the number of dominant modes. To understand how this can happen, consider a simple example in which there are two dominant modes. The analysis of three given, distinct transfer function vectors, denoted $\underset{\sim}{v}_1$, $\underset{\sim}{v}_2$, and $\underset{\sim}{v}_3$, then should indicate two modes. The set of three vectors is linearly dependent, but suppose also that $\underset{\sim}{v}_1$ and $\underset{\sim}{v}_2$ are independent and $\underset{\sim}{v}_1$ and $\underset{\sim}{v}_3$ are dependent. If the transfer function matrix is defined as $[H^*] = [\underset{\sim}{v}_1, \underset{\sim}{v}_2, \underset{\sim}{v}_3]$, then $G^{(1)} = 1$, $G^{(2)} > 0$, and $G^{(3)} = 0$, leading to the correct conclusion that $q = 2$. If, on the other hand, we define $[H^*] = [\underset{\sim}{v}_1, \underset{\sim}{v}_3, \underset{\sim}{v}_2]$, then $G^{(1)} = 1$ and $G^{(2)} = G^{(3)} = 0$, leading to the incorrect conclusion that $q = 1$. An instance of this particular case occurring in a realistic situation is presented in Section IV.3. It is clear that the

ordering of vectors in the p x k transfer function matrix affects all Gramian values except $G^{(1)} = 1$ and $G^{(k)}$, which is invariant with column and row ordering.

The Gramian method then has some serious weaknesses. Perhaps for this reason, it apparently has not been employed widely. The authors have located only one published application, that by Klosterman [7]. The vector-fit method to be discussed next is, to a considerable extent, free of the weaknesses of the Gramian method.

III.3 VECTOR-FIT METHOD

A concept analogous to the number of dominant modes of a vibrating structure is that of a "best approximating subspace". Cliff [8] discussed this concept in the context of control theory. Given a set of k p-dimensional vectors, one can calculate the particular m-dimensional basis ($m < k$) which, among all possible m-dimensional bases, does the best job of approximately spanning the set of k vectors, with error minimized in the least-squares sense. In other words, the k vectors are "fit" to the best approximating m-dimensional subspace. The method developed here to solve for the number of dominant modes follows Cliff's general approach; hence, it is referred to as the vector-fit method.

Given the p x k transfer function matrix [H*] for frequency ω, the general stepwise procedure for application of the vector-fit method is as follows:

1. A particular p-dimensional complex unit vector $\underset{\sim}{u}_1$ is calculated from [H*]. Among all possible unit vectors, $\underset{\sim}{u}_1$ alone has the property of producing the best, in a sense to be defined, set of one-term approximations to the transfer function columns. This set of approximations takes the form

$$\underset{\sim}{H}^*_j \approx C_{j1}\, \underset{\sim}{u}_1, \quad j = 1,2,\cdots, k$$

where the C_{ji} generally are complex constants. Next, the real scalar error $E^{(1)}$ associated with this set of approximations is calculated.

2. A second unit vector $\underset{\sim}{u}_2$ is calculated. It is orthogonal to $\underset{\sim}{u}_1$. Among all possible unit vectors orthogonal to $\underset{\sim}{u}_1$, $\underset{\sim}{u}_2$ alone has the property of producing, in conjunction with $\underset{\sim}{u}_1$, the best set of two-term approximations to the transfer function columns. This set takes the form

$$\underset{\sim}{H}_j^* \approx \sum_{i=1}^{2} C_{ji}\, \underset{\sim}{u}_i,\ j = 1,2,\cdots,\ k$$

Next, error $E^{(2)}$ associated with this set of approximations is calculated.

•
•
•

3. The mth unit vector $\underset{\sim}{u}_m$ is calculated. It is orthogonal to all other $\underset{\sim}{u}_i$, $i = 1,2,\cdots,\ m-1$. Vector $\underset{\sim}{u}_m$ has the property of producing, in conjunction with $\underset{\sim}{u}_1, \underset{\sim}{u}_2,\cdots, \underset{\sim}{u}_{m-1}$, the best set of m-term approximations to the transfer function columns. This set takes the form

$$\underset{\sim}{H}_j^* \approx \sum_{i=1}^{m} C_{ji}\, \underset{\sim}{u}_i,\ j = 1,2,\cdots,\ k$$

Next error $E^{(m)}$ associated with this set of approximations is calculated.

•
•
•

Each step introduces a refinement of the approximation, so the error diminishes in each step, $E^{(m)} \leq E^{(m-1)}$. If, after $m > 1$ steps of this procedure, we find that $E^{(m)} \approx 0$ relative to $E^{(1)}$, then we may reasonably conclude that the set of transfer function vectors is spanned approximately, with very small error, by an m-dimensional basis. According to equation (7), then, there are m

dominant modes at frequency ω, i.e., $q = m$. It is quite unlikely that the vectors $\underset{\sim}{u}_i$ will be identical to the mode shape vectors $\underset{\sim}{\phi}_i^*$ of equation (7), since the $\underset{\sim}{u}_i$ are orthogonal by definition while the $\underset{\sim}{\phi}_i^*$ need not and generally will not be orthogonal. Nonetheless, it is certain that both sets $\underset{\sim}{u}_i$ and $\underset{\sim}{\phi}_i^*$ span the same q-dimensional vector space.

If $p < k$ and the procedure is carried through p steps, then $E^{(p)} \equiv 0$ since the p independent $\underset{\sim}{u}_i$ exactly span p-dimensional space. If, on the other hand, $k < p$ and the procedure is carried through k steps, then $E^{(k)} \equiv 0$ since the k independent $\underset{\sim}{u}_i$ exactly span the subspace defined by the k transfer function column vectors. (This case is simply orthogonalization of a vector set, similar to the Gram-Schmidt procedure.) Hence, in order for the vector-fit method to produce a correct evaluation of the number of dominant modes, it is necessary that p and k each must exceed q. That is, the test engineer must provide both more motion sensors and more excitation stations than the maximum number of dominant modes likely to be encountered. In application, the method itself indicates if too few motion sensors or excitation stations have been used, and this is illustrated in Section IV.3.

It is worthy of note that each of the three methods described for identification of the presence of q dominant modes requires a minimum of q + 1 motion sensors and q + 1 excitation stations.

The theory associated with the calculations discussed above is developed next. Let a basis for p-dimensional space of complex vectors consist of p orthogonal unit vectors $\underset{\sim}{u}_1, \underset{\sim}{u}_2, \cdots, \underset{\sim}{u}_p$, which are unknown at this point. Any transfer function column vector can be expressed as the summation

$$\underset{\sim}{H}_j^* = \left(\sum_{i=1}^{m} + \sum_{i=m+1}^{p} \right) \left(\overline{\underset{\sim}{u}}_i, \underset{\sim}{H}_j^* \right) \underset{\sim}{u}_i, \quad j = 1,2,\cdots, k$$

The basis vectors are orthogonal in the Hermitian sense, so

$$(\bar{\underset{\sim}{H}}_j^{\star}, \underset{\sim}{H}_j) = \left(\sum_{i=1}^{m} + \sum_{i=m+1}^{p} \right) (\bar{\underset{\sim}{u}}_i, \underset{\sim}{H}_j^{\star})(\bar{\underset{\sim}{H}}_j^{\star}, \underset{\sim}{u}_i)$$

Hence, we may define as follows the squared scalar error associated with approximation of $\underset{\sim}{H}_j^{\star}$ as a series sum in only the first m basis vectors,

$$\left(e_j^{(m)}\right)^2 = \sum_{i=m+1}^{p} (\bar{\underset{\sim}{u}}_i, \underset{\sim}{H}_j^{\star})(\bar{\underset{\sim}{H}}_j^{\star}, \underset{\sim}{u}_i)$$

$$= (\bar{\underset{\sim}{H}}_j^{\star}, \underset{\sim}{H}_j^{\star}) - \sum_{i=1}^{m} (\bar{\underset{\sim}{u}}_i, \underset{\sim}{H}_j^{\star})(\bar{\underset{\sim}{H}}_j^{\star}, \underset{\sim}{u}_i)$$

The appropriate total or global error, defined in the least-squares sense over all $\underset{\sim}{H}_j^{\star}$, is

$$E^{(m)} = \left[\sum_{j=1}^{k} \left(e_j^{(m)}\right)^2 \right]^{\frac{1}{2}}$$

$$= \left[\sum_{j=1}^{k} (\bar{\underset{\sim}{H}}_j^{\star}, \underset{\sim}{H}_j^{\star}) - \sum_{j=1}^{k} \sum_{i=1}^{m} (\bar{\underset{\sim}{u}}_i, \underset{\sim}{H}_j^{\star})(\bar{\underset{\sim}{H}}_j^{\star}, \underset{\sim}{u}_i) \right]^{\frac{1}{2}}$$

For given m, we wish to determine the basis vectors $\underset{\sim}{u}_i$ so as to minimize $E^{(m)}$ by maximizing the double-summation term. With a few steps of matrix algebra, that term is cast into the more useful form

$$\sum_{j=1}^{k} \sum_{i=1}^{m} (\bar{\underset{\sim}{u}}_i, \underset{\sim}{H}_j^{\star})(\bar{\underset{\sim}{H}}_j^{\star}, \underset{\sim}{u}_i) = \sum_{i=1}^{m} \bar{\underset{\sim}{u}}_i^{t} [A] \underset{\sim}{u}_i$$

where $[A] = [H^*]\,[\bar{H}^*]^t$ is a p x p Hermitian matrix with p real non-negative eigenvalues $\lambda_1 \geq \lambda_2 \geq \ldots \geq \lambda_p \geq 0$ and p corresponding complex, mutually orthogonal unit eigenvectors $\underset{\sim}{\psi}_1, \underset{\sim}{\psi}_2, \ldots, \underset{\sim}{\psi}_p$. Thus, for given m, we wish to minimize

$$E^{(m)} = \left[\sum_{j=1}^{k} (\bar{\underset{\sim}{H}}_j^*, \underset{\sim}{H}_j^*) - \sum_{i=1}^{m} \bar{\underset{\sim}{u}}_i^t [A]\, \underset{\sim}{u}_i \right]^{1/2}$$

Consider first m = 1. The maximum value assumed by the Hermitian quadratic form $\bar{\underset{\sim}{u}}_i^t[A]\, \underset{\sim}{u}_1$ is equal to the largest eigenvalue λ_1, and this maximum results if $\underset{\sim}{u}_1 = \underset{\sim}{\psi}_1$ (Franklin [9]). Hence, the minimum associated error is

$$E^{(1)}_{\min} = \left[\sum_{j=1}^{k} (\bar{\underset{\sim}{H}}_j^*, \underset{\sim}{H}_j^*) - \lambda_1 \right]^{1/2}$$

Next, for m = 2 we wish to minimize

$$E^{(2)} = \left[\sum_{j=1}^{k} (\bar{\underset{\sim}{H}}_j^*, \underset{\sim}{H}_j^*) - \lambda_1 - \bar{\underset{\sim}{u}}_2^t[A]\, \underset{\sim}{u}_2 \right]^{1/2}$$

For all possible $\underset{\sim}{u}_2$ orthogonal to $\underset{\sim}{u}_1 = \underset{\sim}{\psi}_1$, the maximum value assumed by quadratic form $\bar{\underset{\sim}{u}}_2^t[A]\, \underset{\sim}{u}_2$ is equal to the second eigenvalue λ_2, and this maximum results if $\underset{\sim}{u}_2 = \underset{\sim}{\psi}_2$ (Franklin [9]). Thus,

$$E^{(2)}_{\min} = \left[\sum_{j=1}^{k} (\bar{\underset{\sim}{H}}_j^*, \underset{\sim}{H}_j^*) - \sum_{i=1}^{2} \lambda_i \right]^{1/2}$$

This reasoning can be extended easily to show that the minimum error for arbitrary m ($1 \leq m \leq p$) is

$$E^{(m)} = \left[\sum_{j=1}^{k} (\bar{H}_j^*, H_j^*) - \sum_{i=1}^{m} \lambda_i \right]^{1/2} \qquad (8)$$

where $u_i = \psi_i$. To simplify notation, it is understood in equation (8) and in the discussion and numerical examples to follow that $E^{(m)}$ denotes the minimum error, even though subscript min is deleted.

We can now reiterate and summarize the vector-fit method for determining the number q of dominant modes at a given frequency. From the p x k transfer function matrix [H*], the p x p Hermitian matrix $[A] = [H^*][\bar{H}^*]^t$ is formed. It is necessary that $p \geq q + 1$ and $k \geq q + 1$. Next, the real eigenvalues of [A], $\lambda_1 \geq \lambda_2 \geq \ldots \geq \lambda_p \geq 0$, are calculated. Next, for m = 1, 2, ..., p, the minimum error values are calculated from equation (8). The smallest integer m for which $E^{(m)} \simeq 0$ relative to $E^{(1)}$ then is equal to the number q of dominant modes. Note that the eigenvectors of [A], $\psi_1, \psi_2, \ldots, \psi_p$, need not be calculated.

It can be proved easily that the error values $E^{(m)}$ are entirely independent of the numbering or ordering schemes used to identify motion sensors and exciters or to arrange elements in the transfer function matrix. In other words, any or all of the rows of [H*] can be interchanged and/or any or all of the columns can be interchanged without changing the values of $E^{(m)}$. Hence, the vector-fit method has no weakness comparable to the dependence on vector ordering of the Gramian method.

IV. NUMERICAL SIMULATION STUDY

Two mathematical models have been used for numerical simulation of experimental application of the vector-fit and Gramian methods. The models were designed to have frequency bands of high modal density with prescribed numbers of dominant

modes. The basic objective of the numerical study then was to determine if the vector-fit and Gramian methods are capable of correctly determining the number of dominant modes. Other objectives were to compare the two methods and to develop guidelines for applying the methods and interpreting the results.

To simplify calculations, it was specified that each model have hysteretic damping which does not couple the undamped normal modes. Hence, transfer function matrix elements were calculated exactly from the equation

$$H_{ij} = \sum_{r=1}^{n} \frac{\phi_{ir}\ \phi_{jr}}{M_r \omega_r^2 \left| (1 - \frac{\omega^2}{\omega_r^2}) + i g_r \right|}$$

where ϕ_{ir} is the ith element of the complete mode shape vector $\underline{\phi}_r$, $M_r = \underline{\phi}_r^t [m]\ \underline{\phi}_r$ is the generalized mass of the rth normal mode, and ω_r and g_r are, respectively, the natural frequency and hysteretic damping of the rth mode.

IV.1 TEN-MODE MODEL

The mode shapes of this model are those of the first ten out-of-plane vibration modes of the uniform stretched membrane shown on Figure 1,

$$\phi_{ir} = A_r \sin\left(\frac{m_r \pi x_i}{1.3}\right) \sin\left(\frac{n_r \pi y_i}{1.0}\right)$$

where integers m_r and n_r are the numbers of half-wavelengths for the rth mode listed in Table 1, x_i and y_i are coordinates of the motion sensor/exciter stations shown on Figure 1, and constant A_r for the rth mode is chosen so that the numerically largest mode shape element equals one. Other modal parameters, as listed in Table 1, are not those of the uniform membrane, but rather were selected to produce a mathematical model with four very closely

spaced modes in the vicinity of 100 on the frequency scale and six more modes outside the region of high modal density. Thus, q = 4 in a frequency band of roughly three units centered at 100, so the methods under study, if successful, should indicate accordingly. Since this model has limited physical significance, all quantities are considered to be dimensionless.

IV.2 FIFTEEN-DEGREE-OF-FREEDOM MODEL

This model, unlike the ten-mode model, is based entirely on a physical structure, the cantilevered, rectangular plane grid shown on Figures 2a and b. The model was designed to have two modes with nearly identical natural frequencies, as shown in Table 2. To achieve such close modes, an optimization technique similar to that of Hallauer et al [10] was used.

Each elastic member of the model is a steel bar having Young's modulus E = 200 GPa (29 x 10^6 psi), shear modulus G = 82.7 GPa (12 x 10^6 psi), and diameter of 6.35 mm (0.25 inch). (The fundamental units of pounds, inches, and seconds were used in all calculations.) Each bar may twist about its axis and bend out of the grid plane, and each is clamped at both ends by either the rigid support wall or a rigid cylindrical joint member of 0.051-m (2-inch) diameter. The five node points of the model are the intersections of the bar centerlines in the grid plane. The fifteen degrees of freedom then consist of one out-of-plane translation and two out-of-plane rotations of each node point. The translations are identified in Figure 2a, and the rotations of node 1, for example, are identified in Figure 2b. The nodal lumped mass and moment of inertia (for both rotational dof) associated with each rigid joint are listed in Table 2. To account approximately for distributed inertia of the bars, finite element consistent mass matrices were used, with bar density taken to be 7859 kg/m^3

(7.3536×10^{-4} lb-sec^2/in^4). Modal hysteretic damping constants g_r were specified to be 0.015 for modes 1 and 2, 0.018, 0.022, and 0.026 respectively for modes 3, 4, and 5, 0.03 for modes 6-10, and 0.035 for modes 10-15.

IV.3 RESULTS AND DISCUSSION

Consider first the ten-mode model. Typical transfer functions are shown on Figures 3a and b, with the coincident (co) or real parts and the quadrature (quad) or imaginary parts plotted separately. Qualitative inspection of these and other transfer functions seems to indicate the presence of only two dominant modes in the vicinity of frequency 100. But there are actually four dominant modes in that region, as listed in Table 1.

To begin numerical application of the vector-fit method, we examine first errors calculated from the complete 10 x 10 transfer function matrix. Such a large matrix will not generally be required, but examining this case first establishes a reference and provides guidelines for interpreting the error values and, more generally, for applying the method. Since transfer functions are usually plotted versus excitation frequency, it seems natural and, in fact, proves advantageous also to calculate and plot error values versus excitation frequency. Errors $E^{(m)}$, $m = 1,2,\cdots,10$, for the complete transfer function matrix were calculated from equation (8) and are plotted on Figure 4. Note the relatively large variations with frequency and the peaking of $E^{(1)}$, $E^{(2)}$, and $E^{(3)}$. Note also that $E^{(4)}$ is on the order of 10% of the maximum value of $E^{(1)}$, and that $E^{(4)}$ varies only slightly with frequency. As stated in Section III.3, the result that $E^{(4)} << E^{(1)}$ indicates that there are four dominant modes. But it is also important that $E^{(4)} \neq 0$ and that $E^{(4)}$, $E^{(5)}$, etc. vary slowly with frequency in comparison with $E^{(1)}$, $E^{(2)}$, and $E^{(3)}$. From these observations, we conclude that four modes dominate

but do not completely describe the response in this narrow frequency band, and that the contributions of distant modes remain relatively constant in this band. Both conclusions are quite reasonable in view of the nature of the ten-mode model. Thus, this reference case suggests that in examining graphs of error versus frequency, we should use not only the basic criterion $E^{(q)} << E^{(1)}$, but also the additional criteria that $E^{(q)} \neq 0$, that $E^{(q)}$, $E^{(q+1)}$, etc. should vary slowly with frequency in comparison with $E^{(1)}$, $E^{(2)}$, ..., $E^{(q-1)}$, and that plots versus frequency of $E^{(1)}$, $E^{(2)}$,..., $E^{(q-1)}$ should exhibit peaks. An exceptional case for which these criteria might not apply is that of a distant mode contributing significantly to response. In this case, we might expect to find a relatively large, slowly varying, and non-peaking $E^{(m)}$ for $m < q$.

Figures 5 a-d are plots of errors calculated from responses at seven motion sensor locations due successively to excitation at three, four, five and six locations. This simulates a realistic testing approach in which very few exciters are applied initially, and additional exciters are applied as required. In Figure 5a for three exciters, $E^{(2)}$ is not much smaller than $E^{(1)}$, and $E^{(3)} = 0$, as required by the theory of Section III.3. (The very small non-zero values on this and other computer-generated plots are due to round-off errors.) Clearly, more exciters are required to indicate correctly the number of dominant modes. The addition of a fourth exciter (i.e., another column in $[H^*]$) leads to Figure 5b, which also indicates the need for at least one more exciter. With five exciters, however, Figure 5c shows that $E^{(4)}$ varies slowly with frequency and is non-zero yet much smaller than $E^{(1)}$. We conclude, therefore, that $q = 4$. Figure 5d for six exciters substantiates the conclusion.

Unfortunately, interpretation of the error plots is not always as

unambiguous as it appears to be with Figures 4 and 5. There is a definite dependence on the motion sensor and exciter locations represented in the transfer function matrix. These points are illustrated on the error plots of Figures 6 a,b, and c, which were calculated for different sets of motion sensor/exciter locations than those of Figures 4 and 5. Figure 6a for five motion sensors and five exciters can be interpreted as indicating four dominant modes; but this interpretation is substantially weaker here than for Figures 4 and 5c,d since $E^{(3)}$ on Figure 6a is only slightly peaked and is very small relative to $E^{(1)}$. Figure 6b for six motion sensors and six exciters is ambiguous; one might infer that it indicates three, four, or five dominant modes, with three being perhaps the most likely interpretation. Figure 6c, also with six motion sensor/exciter locations but one different location than Figure 6b, permits a somewhat more certain interpretation of four dominant modes.

One can observe from the vertical axis scales on Figures 4 - 6 that all non-zero error values tend to increase as columns are added to the transfer function matrix. This tendency appears not to have any useful significance.

Next, we examine the Gramian method as applied to the ten-mode model. Figure 7a is a graph of Gramians plotted versus frequency in the region of high modal density. Gramians $G^{(1)}$ - $G^{(10)}$ were calculated from complete 10 x 1 transfer function vectors, with the vectors applied in the order of the station numbering shown on Figure 1, i.e., 1, 2, ..., 10. Recall that the identification criterion for this method is $G^{(q+1)} \approx 0$, where $G^{(1)} = 1$ by virtue of transfer function vector normalization. So $G^{(5)}$ should be nearly zero in this

case. A tabulation of $G^{(5)}$ for Figure 7a (not included) shows values in the ranges 10^{-3} and 10^{-4}. Figure 7b is a graph of Gramians $G^{(1)}$ - $G^{(10)}$ also calculated from 10 x 1 transfer function vectors, but with the vectors applied in inverse order of the station numbering, i.e., 10, 9,...,1. Values of $G^{(5)}$ for Figure 7b are in the ranges 10^{-1} and 10^{-2}. The vast differences between the curves on Figure 7a and those on Figure 7b illustrate the vector-ordering dependence of the Gramian method, and the different magnitudes of $G^{(5)}$ on the two graphs illustrate the indefiniteness of the smallness criterion, $G^{(q+1)} \approx 0$.

Finally for the ten-mode model, Figures 8a and b demonstrate the significance on typical transfer function plots of the dominance of four modes. These graphs show exact coincident and quadrature values of $H_{3,3}(\omega)$ and $H_{7,7}(\omega)$, approximate values calculated from only the four dominant modes, and approximate values calculated from only modes four and six, two of the dominant modes. Whereas modes four and six alone dominate $H_{3,3}$, all four of the close modes make comparable contributions to $H_{7,7}$.

Consider next the fifteen-dof model, which has the pair of close modes listed in Table 2. In testing of this model, it would be natural to instrument and to provide forcing excitation at the five translation degrees of freedom shown on Figure 2a, so we will analyze the 5 x 5 incomplete transfer function matrix associated with those degrees of freedom.

Figures 9a,b, and c are selected transfer functions in a narrow band about the close natural frequencies. Figure 9a for $H_{1,1}(\omega)$ has the character of most transfer function elements in this frequency band, namely, it seems to indicate only a single, isolated mode. Figure 9b for $H_{4,10}(\omega)$ suggests the presence of more than one mode, but the asymmetry of the coincident response

curve would probably be attributed to a distant mode rather than to close modes. Of all the elements of the 5 x 5 [H*], only $H_{1,13}(\omega)$ shown on Figure 9c provides definite evidence of the presence of two close modes. But both $H_{4,10}$ and $H_{1,13}$ have such small magnitudes relative to $H_{1,1}$ that, in actual testing, they would probably be lost in noise or ignored. So it is fair to say that qualitative examination of the transfer functions indicates the presence of only a single mode at 149.2 rad/sec.

Before examining error plots in the region of the two close modes, it is useful to have as a reference an example of error plots at and near a single isolated mode. The second mode of this model, with a natural frequency of 67.5 rad/sec, is quite distant from all other modes. Figure 10a is the graph of error values around this mode for the 5 x 5 [H*]. For comparison, Figure 10b is the graph of error values in a region of almost no modal activity between the second and third modes. The error scales of both Figures 10a and b are quite small (relative to that of Figure 11a discussed below), and neither figure has any error peaks. The only significant difference in character between the two figures is the numerical noise at and near the natural frequency in Figure 10a, due to accumulated round-off error in eigenvalue calculations.

Figures 11a and b are graphs of error values in a band around the pair of close modes, the former for excitation at all five translation degrees of freedom, and the latter for excitation at only three. On the basis of all criteria developed previously and in comparison with Figure 10a, these graphs indicate clearly and indisputably the presence of two dominant modes.

Figures 12 a, b, and c are graphs of Gramians in the region of close modes. Figure 12a for five exciters applied in the order 1, 4, 7, 10, 13 seems to

indicate clearly that q = 2. So also does Figure 12b for three exciters applied in the order 13, 1, 10. However, Figure 12c for the same three exciters applied in the order 1, 10, 13 seems to indicate just as clearly, though incorrectly, that q = 1.

In summary of the discussion of theory and the numerical simulation study, the vector-fit method is distinctly superior to the Gramian method for the purpose of determining the number of dominant modes. The only advantage of the Gramian method is that it requires substantially less computation time. As has been demonstrated, the vector-fit method can produce error plots which are difficult to interpret correctly. But results of the simulation study suggest that the use of a large number of motion sensors in calculation of the error values will reduce the likelihood of mistaken interpretations. Theoretically, a minimum number of q+1 motion sensors are required; however, it would seem prudent and usually practical to estimate q and then to use several times that number of motion sensors in calculating error values.

We note that the vector-fit method is valid regardless of the type of motion sensor employed in testing, since the form of equation (7) remains the same for displacement, velocity, or acceleration transfer functions.

V. CONCLUDING REMARKS

The vector-fit method for determining the number of dominant vibration modes from structural transfer functions has been derived theoretically, illustrated with a numerical simulation study, and compared with other methods. The method works well with exact, noiseless, simulated data. However, its practical applicability has not been evaluated. The logical next step is to test the method

with real data. If it should prove applicable, it would be a useful analysis tool for modal testing. Regardless of the type of testing employed, the vector-fit method could provide an independent check on whether or not all significant modes had been detected.

ACKNOWLEDGEMENTS

This work has been sponsored by NASA Langley Research Center under Research Grant NSG 1276. The authors are most grateful to E. M. Cliff, who contributed the theoretical basis for the vector-fit method from his research in control theory, and to Paul Conti, who assisted in the study.

BASIC NOTATION

$(\underset{\sim}{\ })$	column matrix, vector
Re( )	real part of ( )
$[\ ]^t$, $(\underset{\sim}{\ })^t$	transpose of [ ], $(\underset{\sim}{\ })$
$\overline{(\ )}$	complex conjugate of ( )
det [ ]	determinant of [ ]
$(\underset{\sim}{u},\underset{\sim}{v}) = \underset{\sim}{\bar{u}}^t\underset{\sim}{v}$	Hermitian scalar product
$[A] = [H^*]\,[\bar{H}^*]^t$	p x p Hermitian matrix
[c]	n x n damping matrix
$[G_k] = [\bar{H}^*]^t\,[H^*]$	k x k Gram matrix
[H]	n x n transfer function matrix
[H*]	p x k incomplete transfer function matrix
[k]	n x n stiffness matrix
[m]	n x n inertia matrix
$[\phi]$	n x n modal matrix
[S]	an unspecified n x n complex matrix
F	force-amplitude vector
$\underset{\sim}{H}_j$	jth column of [H]
$\underset{\sim}{H}^*_j$	jth column of [H*]
ϕ_r	rth column of $[\phi]$
$\underset{\sim}{\phi}^*_r$	p x 1 sub-vector of $\underset{\sim}{\phi}_r$
$\underset{\sim}{\psi}_i$	ith complex unit eigenvector of [A]
$\underset{\sim}{u}_i$	p x 1 complex unit basis vector
$\underset{\sim}{x}(t)$	n x 1 time-dependent response vector
$\underset{\sim}{X}$	n x 1 complex response-amplitude vector
C_{ij}	unspecified complex constant

$E^{(m)}$	mth real error value
$G^{(k)} = \det[G_k]$	Gram determinant, Gramian
g_r	hysteretic damping constant of rth mode
$i = \sqrt{-1}$	
k	number of dof subjected to forcing excitation
λ_i	ith eigenvalue of [A]
M_r	generalized mass of rth normal mode
m_r, n_r	numbers of half-wavelengths for the ten-mode model
n	total number of dof
ω	frequency of excitation
ω_r	natural frequency of rth normal mode
p	number of dof instrumented with motion sensors
q	number of dominant modes
S_{ij}	element of [S]

REFERENCES

1. Traill-Nash, R. W., "On the Excitation of Pure Natural Modes in Aircraft Resonance Testing", J. Aero/Space Sci., Dec. 1958, pp. 775-778.

2. Bishop, R. E. D. and Gladwell, G. M. L., "An Investigation into the Theory of Resonance Testing", Phil. Trans. of the Royal Society of London, Series A, Vol. 255, Math. and Phys. Sci., 1963, pp. 241-280.

3. Asher, G. W., "A Note on the Effective Degrees of Freedom of a Vibrating Structure", AIAA Journal, Vol. 5, No. 4, April 1967, pp. 822-824.

4. Meirovitch, L., Elements of Vibration Analysis, McGraw-Hill, 1975, Chapter 4.

5. Ibrahim, S. R. and Mikulcik, E. C., "The Experimental Determination of Vibration Parameters from Time Responses", The Shock and Vibration Bulletin, Bulletin 46, Part 5, 1976, pp. 187-193.

6. Hildebrand, F. B., Methods of Applied Mathematics, 2nd ed., Prentice-Hall, 1965, Chapter 1.

7. Klosterman, A. L., "On the Experimental Determination and Use of Modal Representations of Dynamic Characteristics", Ph.D. Dissertation, University of Cincinnati, 1971.

8. Cliff, E. M., "Essential Uncontrollability of Discrete Linear, Time-invariant, Dynamical Systems", Proceedings of the IFAC 75, International Federation of Automatic Control, 6th World Congress, August 24-30, 1975, Boston/Cambridge, Mass., Part 1, Section 9.3, pp. 1-6, 1975.

9. Franklin, J. N., Matrix Theory, Prentice-Hall, 1968, Chapter 6.

10. Hallauer, W. L. Jr., Weisshaar, T. A., and Shostak, A. G., "A Simple Method for Designing Structural Models with Closely Spaced Modes of Vibration", scheduled for publication in J. Sound and Vibration, Vol. 61, No. 2, Nov. 1978.

TABLE 1

Parameters of ten-mode model

r	1	2	3	4	5	6	7	8	9	10
ω_r	67.6	82.0	91.2	98.9	99.4	100.1	101.4	110.7	117.6	132.3
g_r	0.015	0.017	0.017	0.021	0.019	0.023	0.024	0.026	0.027	0.03
M_r	0.02	0.009	0.01	0.012	0.011	0.01	0.009	0.011	0.013	0.009
m_r,n_r	1,1	2,1	1,2	3,1	2,2	3,2	1,3	4,1	2,3	4,2

TABLE 2

Inertia parameters and close modes of fifteen-dof model

	Inertia parameters		Close modes		
	Mass	Moment of inertia	r	3	4
Node	kg	10^{-3} kg-m^2	ω_r(r/s)	149.18	149.22
1	0.5114	0.5570	$\phi_{1,r}$	1.000	1.000
2	1.4994	1.7199	$\phi_{4,r}$	0.031	-0.274
3	2.0390	4.1627	$\phi_{7,r}$	0.446	-0.444
4	0.4756	0.1154	$\phi_{10,r}$	-0.421	-0.236
5	2.0424	4.1833	$\phi_{13,r}$	-0.151	0.216

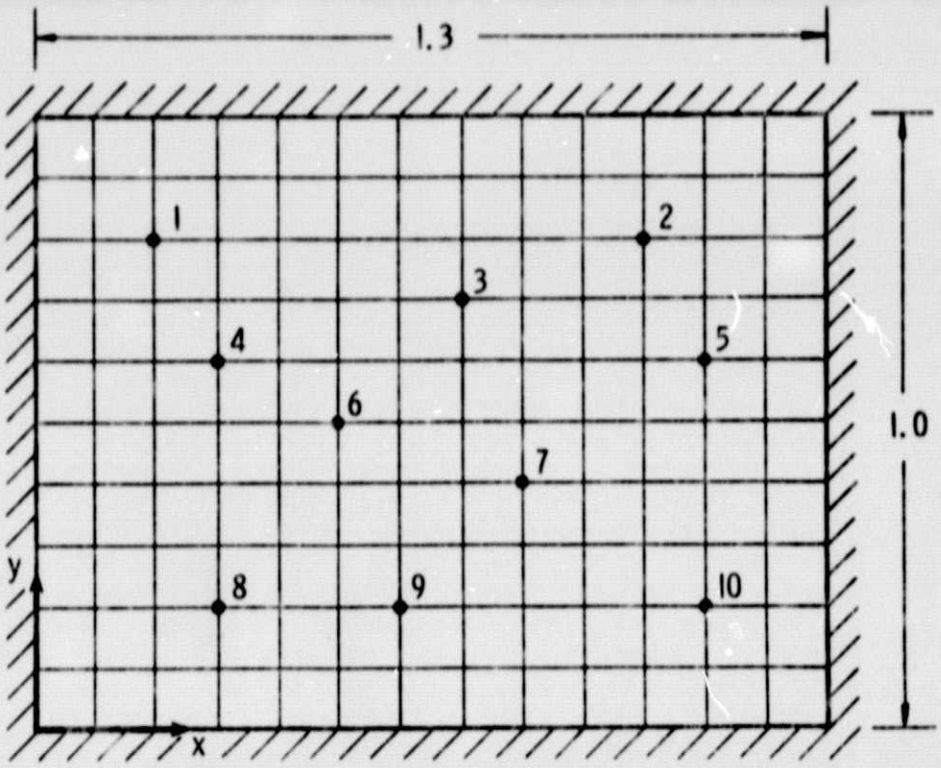

Fig. 1 Stretched membrane for mode shapes of ten-mode model

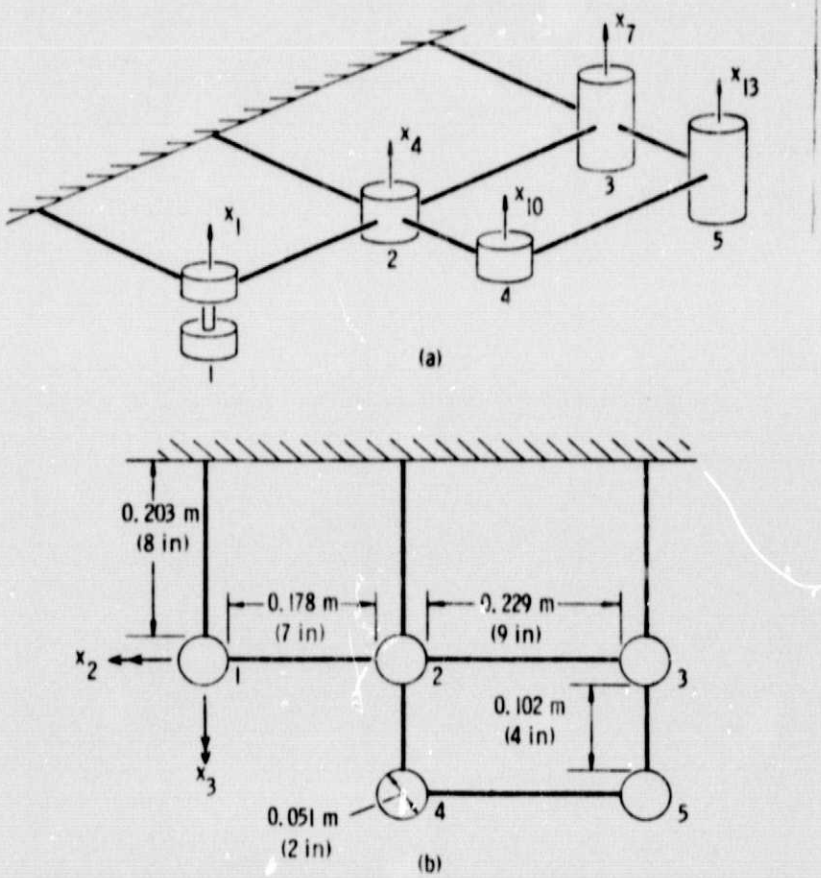

Figs. 2 Fifteen-degree-of-freedom model: (a) pictorial view with translation dof; (b) plan view

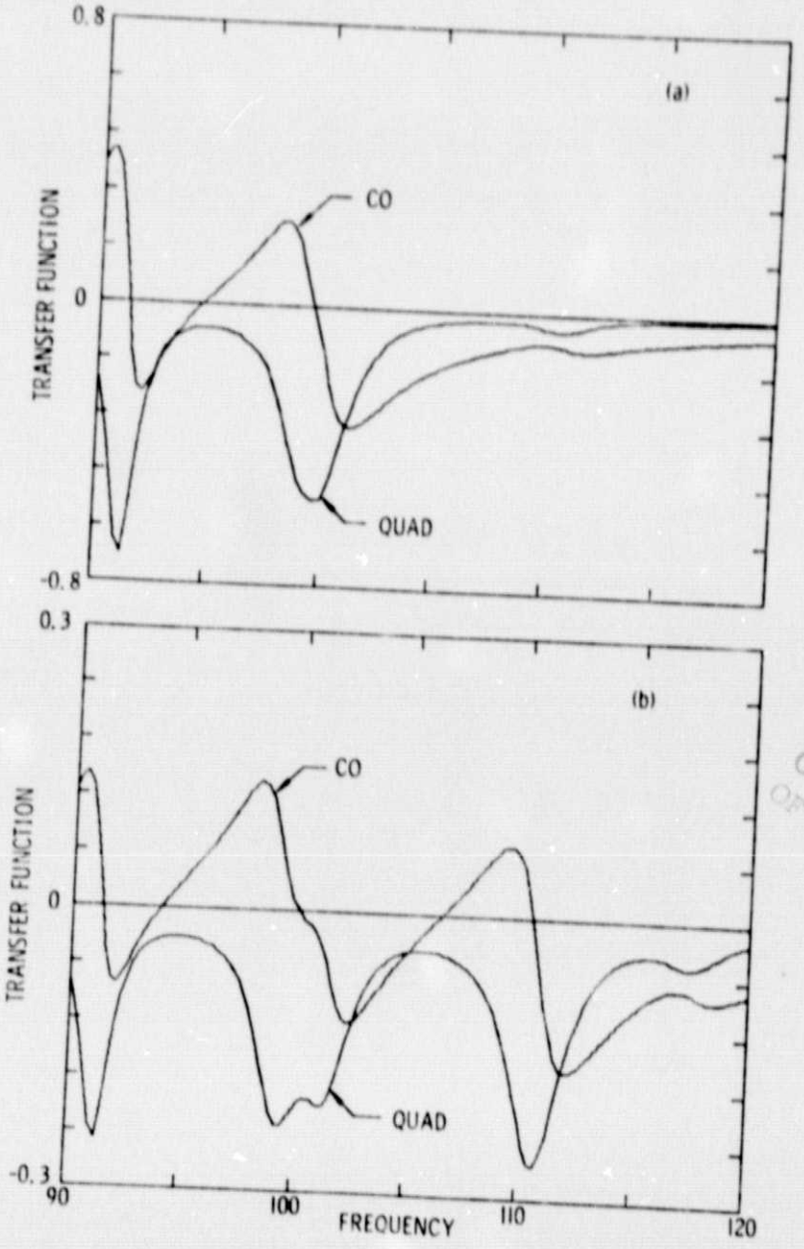

Figs. 3 Typical transfer functions for the ten-mode model: (a) $H_{3,3}(\omega)$; (b) $H_{7,7}(\omega)$

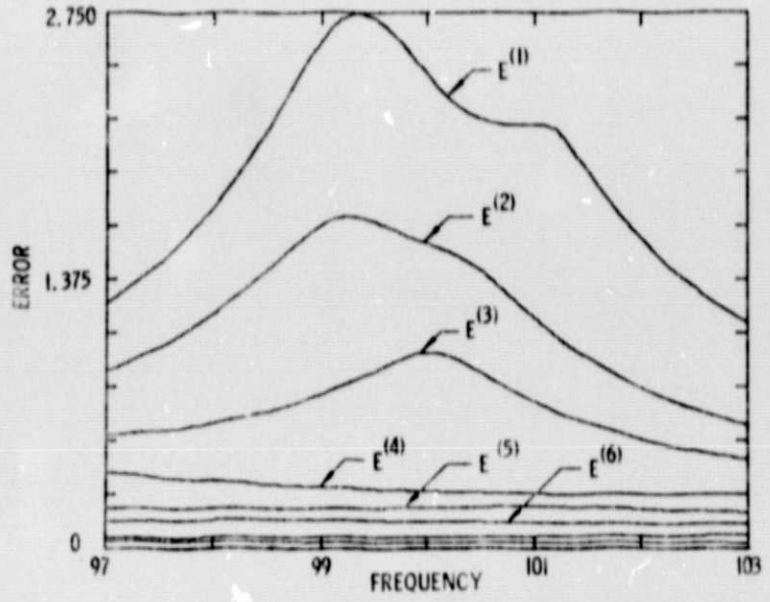

Fig. 4 Reference error graph for the ten-mode model with all motion sensors and all exciters

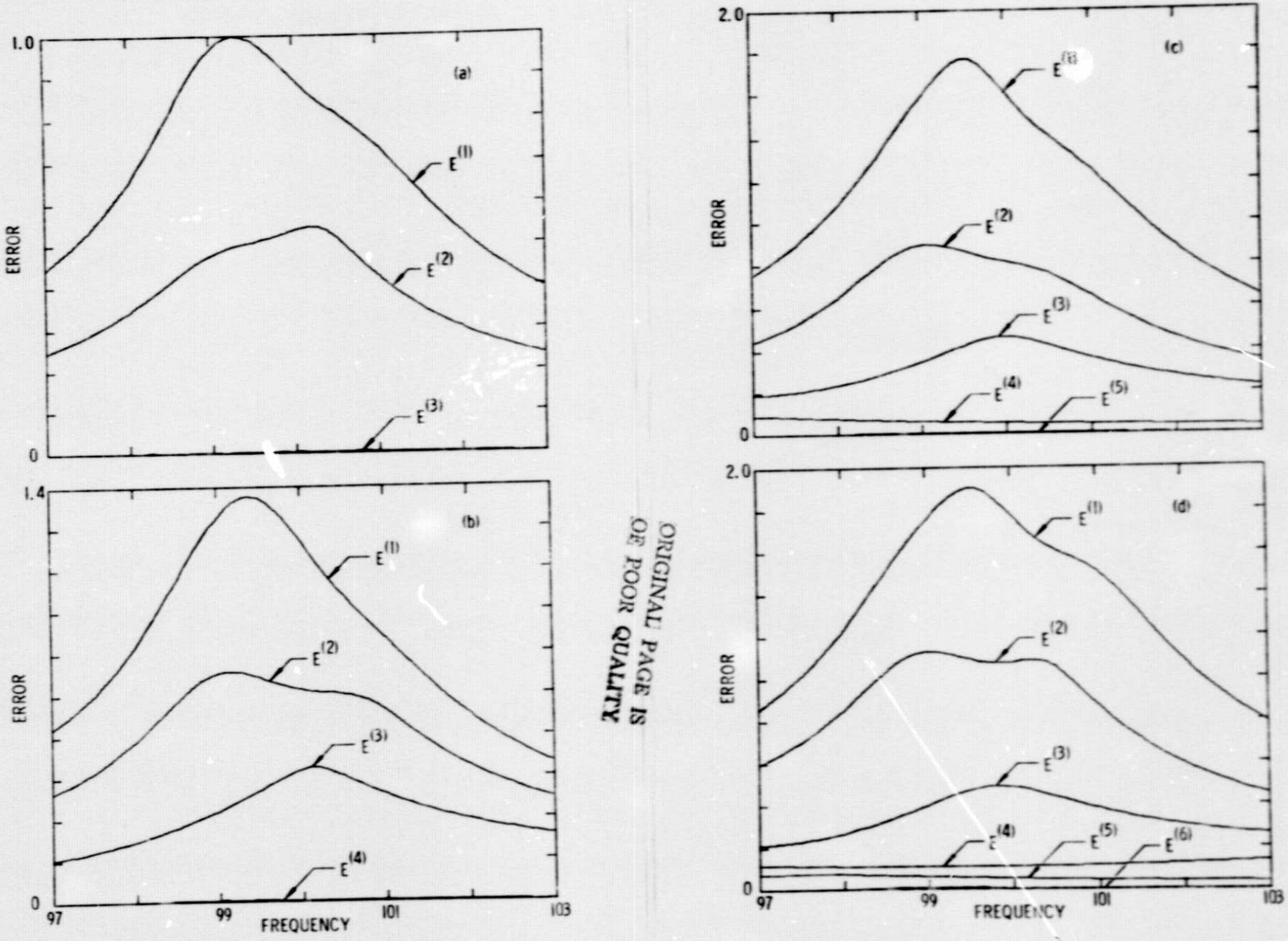

Figs. 5 Error graphs for the ten-mode model with motion sensors 1, 2, 5, 6, 8, 9, 10: (a) exciters 1, 6, 9; (b) exciters 1, 2, 6, 9; (c) exciters 1, 2, 6, 8, 9; (d) exciters 1, 2, 6, 8, 9, 10

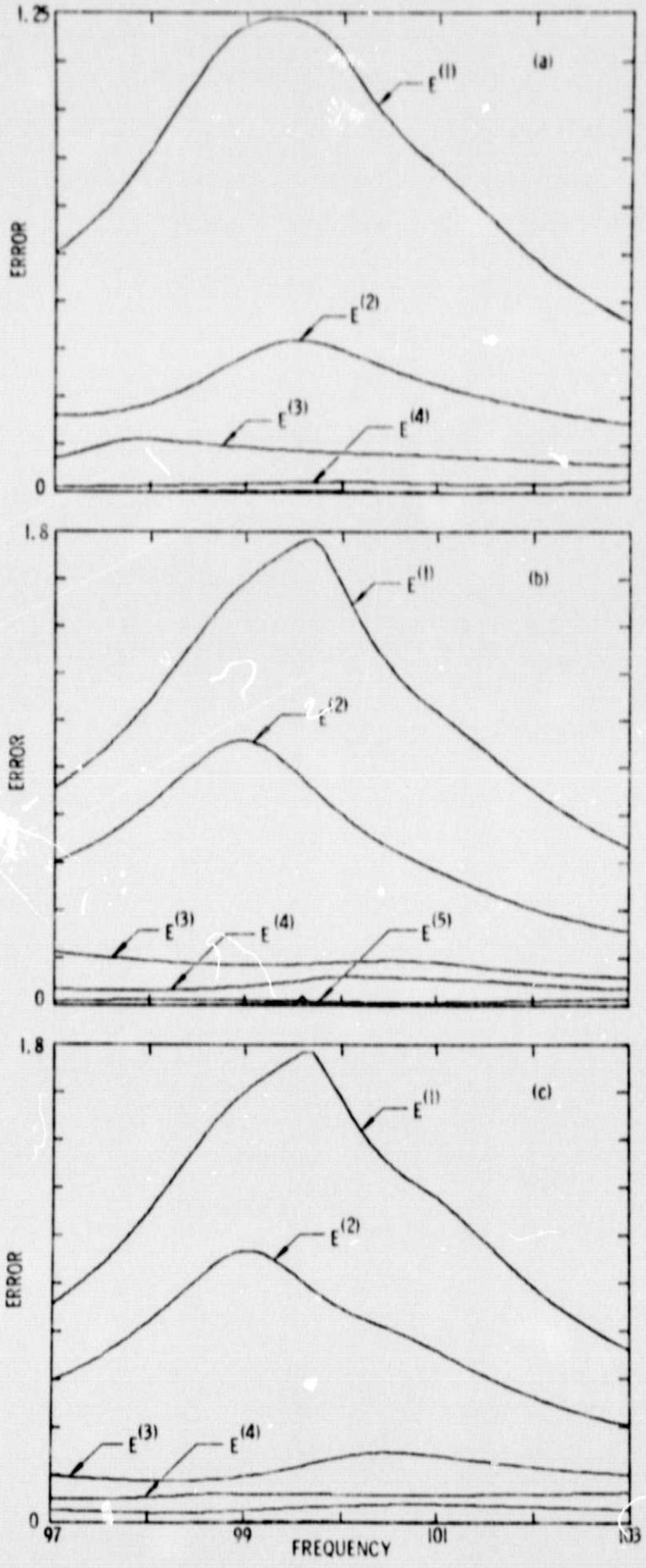

Figs. 6
Error graphs for the ten-mode model (a) motion sensors/exciters 2, 3, 4 7, 8; (b) motion sensors/exciters 2 3, 4, 7, 8, 10; (c) motion sensors/ exciters 2, 3, 4, 6, 8, 10

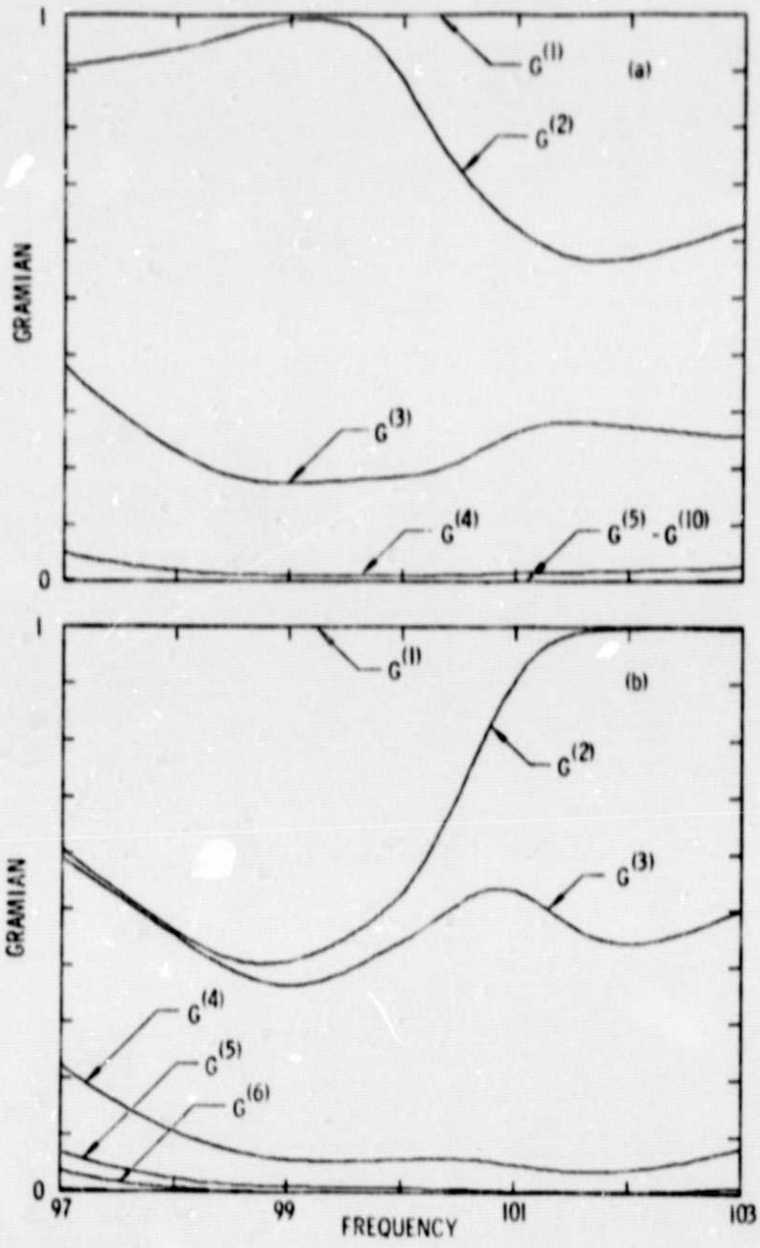

Figs. 7 Gramian graphs for the ten-mode model with all ten motion sensors: (a) all ten exciters applied in forward order, 1, 2, . . . , 10; (b) all ten exciters applied in reverse order, 10, 9, . . . , 1

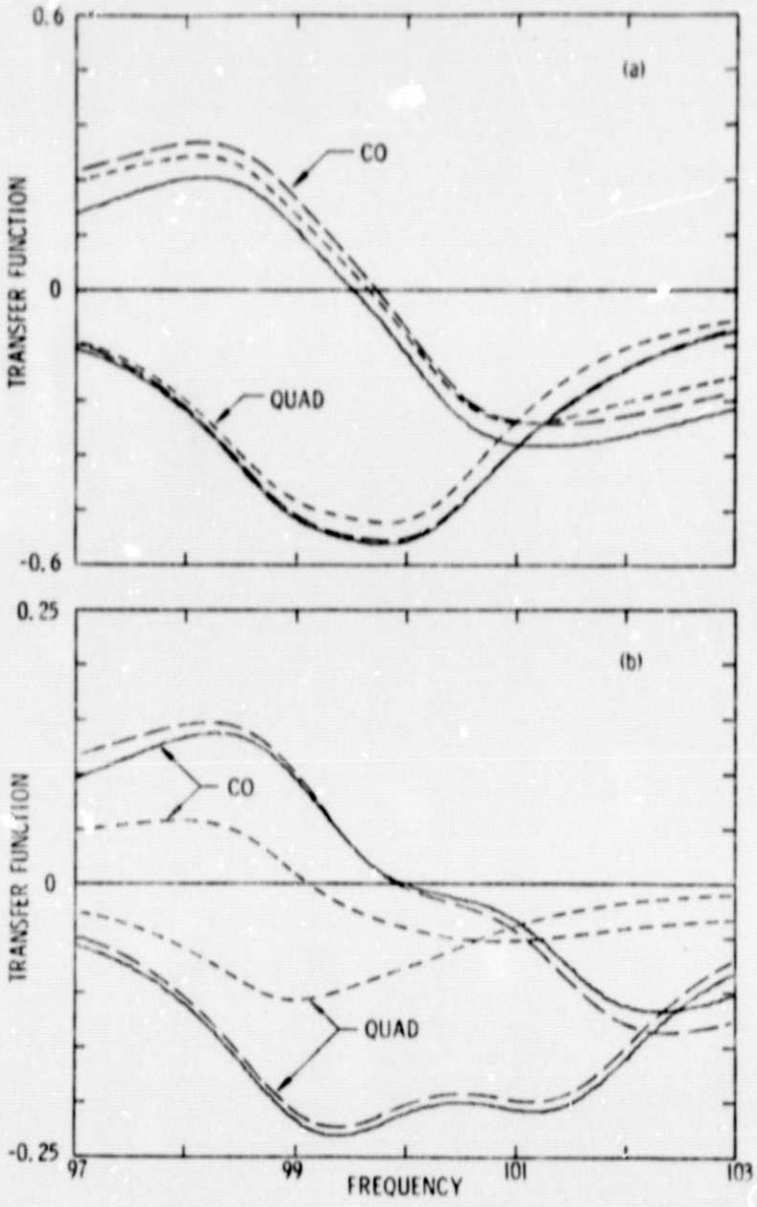

Figs. 8 Comparisons of exact and approximate transfer functions for the ten-mode model, with solid lines for exact values, long dashes for modes 4, 5, 6, and 7, and short dashes for modes 4 and 6: (a) $H_{3,3}(\omega)$; (b) $H_{7,7}(\omega)$

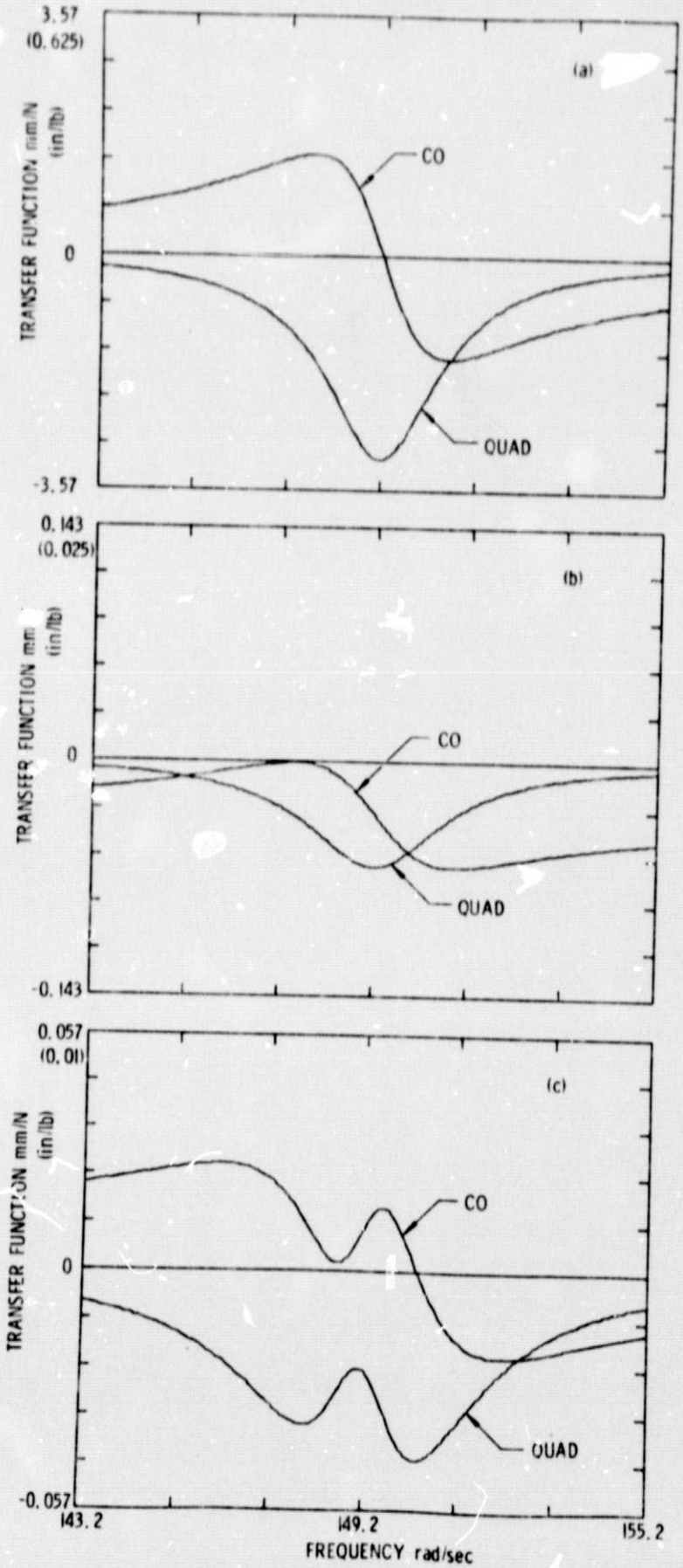

Figs. 9
Transfer functions for the fifteen-dof model: (a) $H_{1,1}(\omega)$; (b) $H_{4,10}(\omega)$
(c) $H_{1,13}(\omega)$

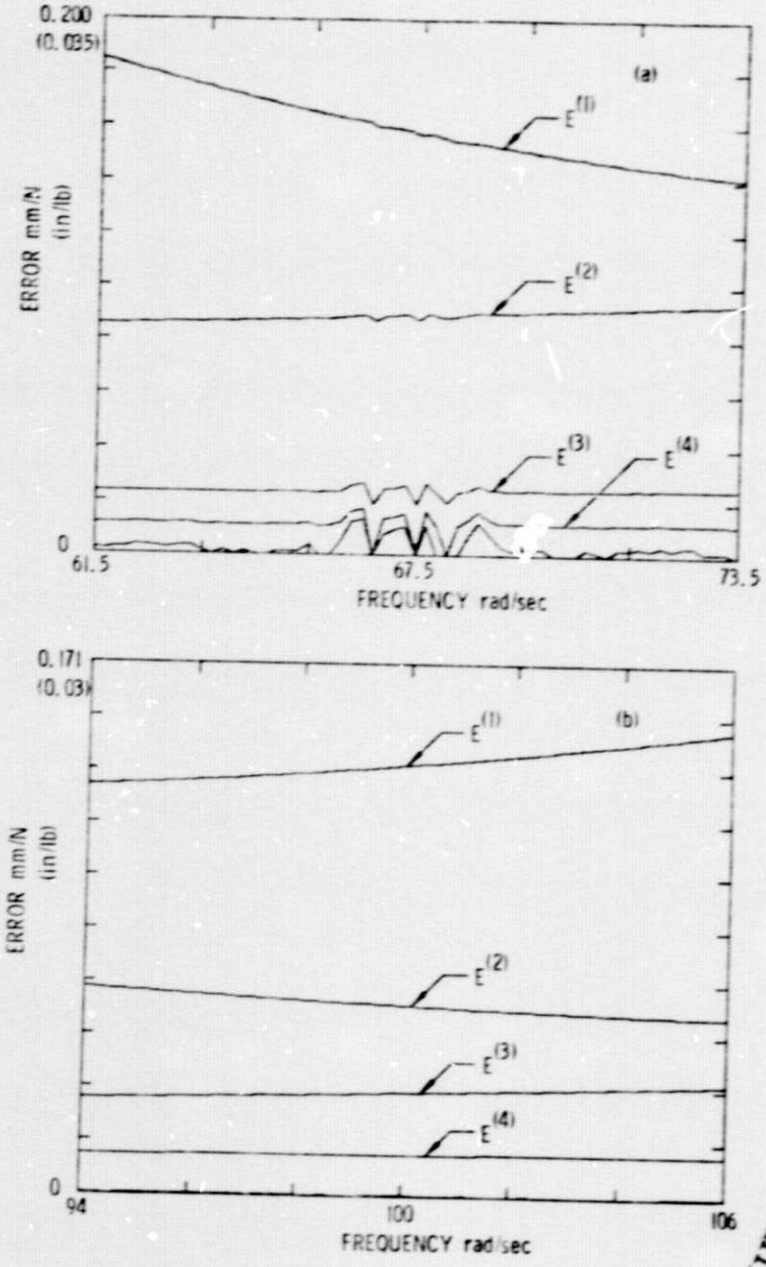

Figs. 10 Error graphs for the fifteen-dof model with motion sensors/exciters 1, 4, 7, 10, 13: (a) in the region of a single isolated mode; (b) in a region of very little modal activity

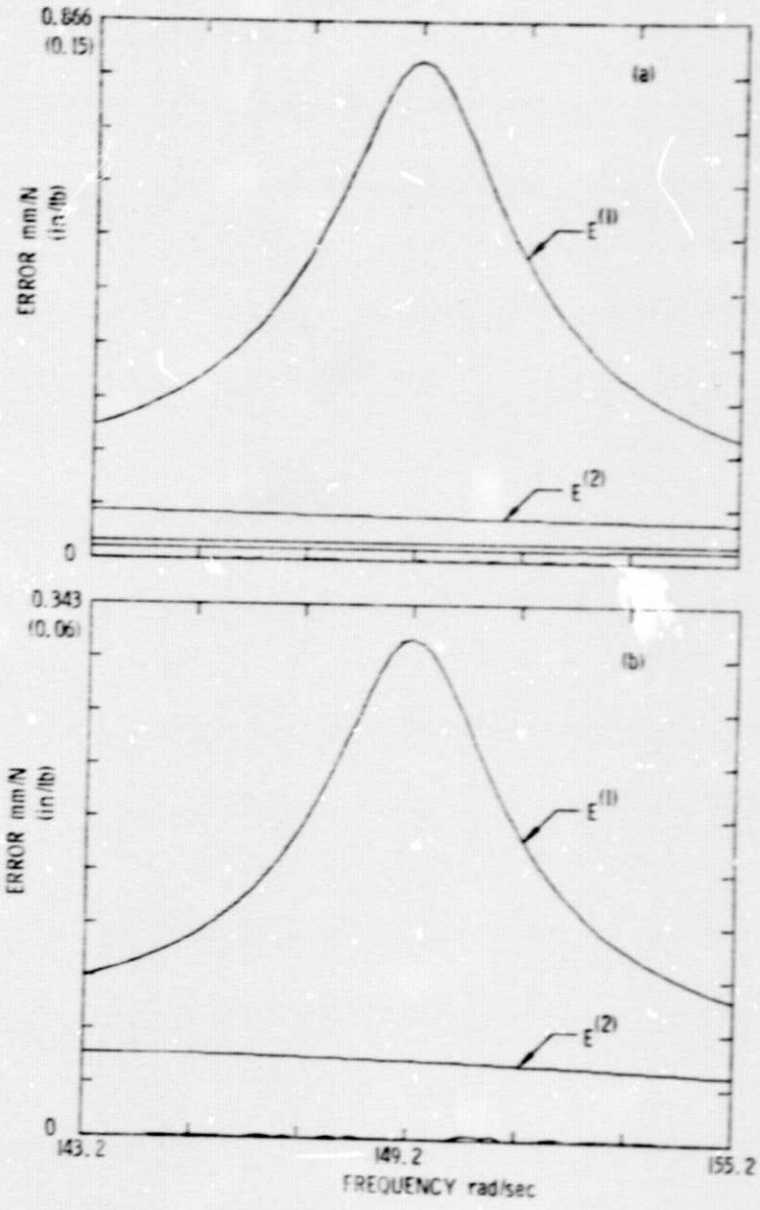

Figs. 11 Error graphs for the fifteen-dof model with motion sensors 1, 4, 7, 10, 13: (a) exciters 1, 4, 7, 10, 13; (b) exciters 1, 10, 13

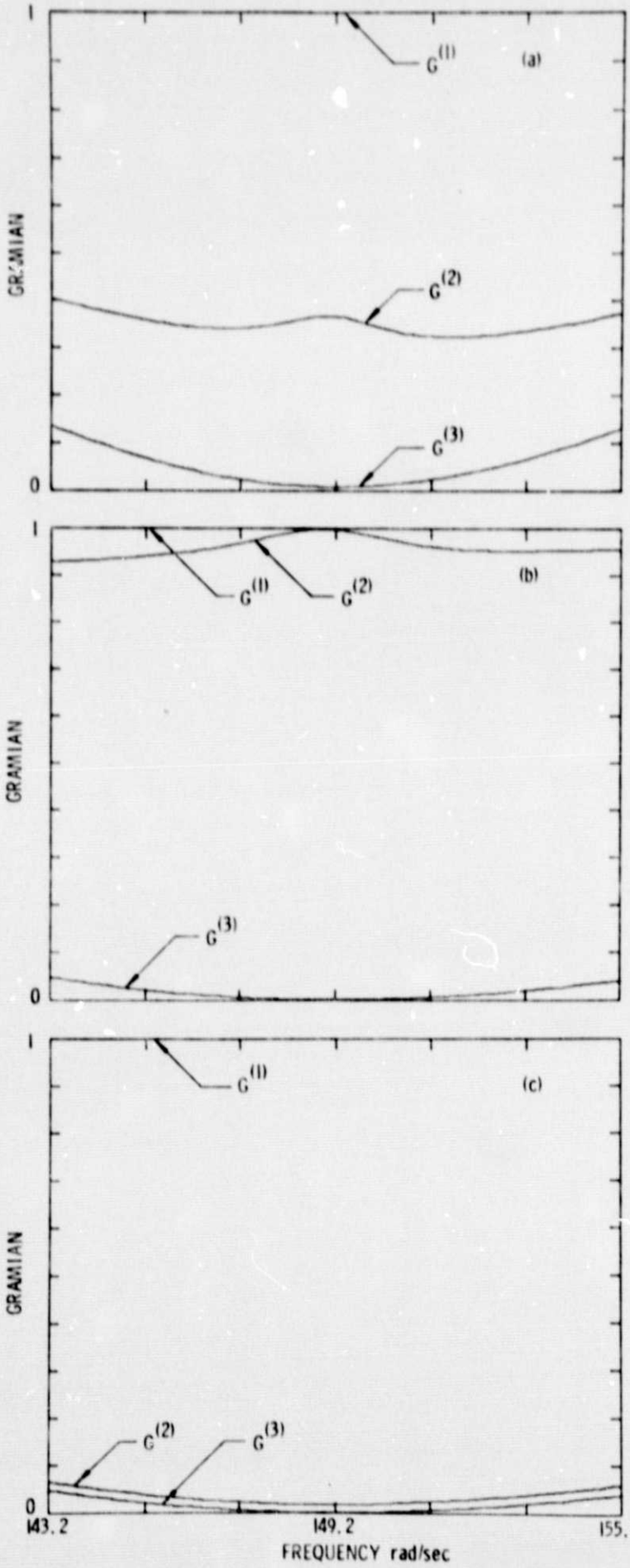

Figs. 12
Gramian graphs for the fifteen-dof model with motion sensors 1, 4, 7, 10, 13: (a) five exciters applied in the order 1, 4, 7, 10, 13; (b) three exciters applied in the order 13, 1, 10; (c) three exciters appli in the order 1, 10, 13